

1 **MELTS\_Excel: A Microsoft Excel-based MELTS interface for research and**  
2 **teaching of magma properties and evolution**

3 Guilherme A. R. Gualda, Earth & Environmental Sciences, Vanderbilt University, Nashville,  
4 Tennessee, USA.

5 Mark S. Ghiorso, OFM Research - West, Seattle, Washington, USA.

6

7

8

9

10

11

12

13

14

15

16

17

18

19

20

21

22

23

24

25 Corresponding author: G. A. R. Gualda, Earth & Environmental Sciences, Vanderbilt University,  
26 Nashville, TN 37235, USA. ([g.gualda@vanderbilt.edu](mailto:g.gualda@vanderbilt.edu))

27 **Key points**

- 28 • Rhyolite-MELTS interface based on Microsoft Excel

29 **Abstract**

30 The thermodynamic modeling software MELTS is a powerful tool for investigating crystallization  
31 and melting in natural magmatic systems. Rhyolite-MELTS is a recalibration of MELTS that  
32 better captures the evolution of silicic magmas in the upper crust. The current interface of  
33 rhyolite-MELTS, while flexible, can be somewhat cumbersome for the novice. We present a new  
34 interface that uses web services consumed by a VBA backend in Microsoft Excel<sup>®</sup>. The interface  
35 is contained within a macro-enabled workbook, where the user can insert the model input  
36 information and initiate computations that are executed on a central server at OFM Research.  
37 Results of simple calculations are shown immediately within the interface itself. It is also  
38 possible to combine a sequence of calculations into an evolutionary path; the user can input  
39 starting and ending temperatures and pressures, temperature and pressure steps, and the  
40 prevailing oxidation conditions. The program shows partial updates at every step of the  
41 computations; at the conclusion of the calculations, a series of data sheets and diagrams are  
42 created in a separate workbook, which can be saved independently of the interface.  
43 Additionally, the user can specify a grid of temperatures and pressures and calculate a phase  
44 diagram showing the conditions at which different phases are present. The interface can be  
45 used to apply the rhyolite-MELTS geobarometer. We demonstrate applications of the interface  
46 using an example early-erupted Bishop Tuff composition. The interface is simple to use and  
47 flexible, but it requires an internet connection. The interface is distributed for free from  
48 [melts.ofm-research.org](http://melts.ofm-research.org).

49 **Index terms**

50 1011, 3611, 8411, 1009, 3610, 8410, 3618, 3619, 1065

51 **Keywords**

52 Rhyolite-MELTS, thermodynamics, phase equilibria, software

53

## 54 **1. Introduction**

55 The thermodynamic modeling software MELTS [*Ghiorso and Sack, 1995; Asimow and Ghiorso,*  
56 *1998*] and its derivatives [e.g. pMELTS, *Ghiorso et al., 2002*] comprise a powerful and much  
57 utilized set of tools for investigating crystallization and melting in natural magmatic systems  
58 [e.g. *Ghiorso, 1997; Ghiorso and Gualda, 2015*]. Rhyolite-MELTS [*Gualda et al., 2012a*] is a  
59 recent recalibration of MELTS aimed at better capturing the evolution of silicic magmas present  
60 in upper crustal systems (up to ~400 MPa pressure), while maintaining the fidelity of the  
61 original calibration to mafic and alkalic systems. Rhyolite-MELTS also includes many algorithmic  
62 modifications that improve computational performance when compared to MELTS [*Ghiorso,*  
63 *2013*].

64 Currently, most users of MELTS, pMELTS, and rhyolite-MELTS rely on a graphical user interface  
65 (GUI) that runs on UNIX/LINUX-based systems, primarily Intel-based Mac OS X computers. One  
66 of the difficulties with deployment of the GUI is that it has to be built for each of the several  
67 existing computer architectures and operating systems. Also, while the GUI provides a powerful  
68 and flexible interface, the many options available in the GUI lead to a relatively steep learning  
69 curve for the novice user. Finally, there is currently no graphical output of the simulation  
70 results, and the output from the GUI is in the form of text files that need to be processed  
71 offline. For all these reasons, while MELTS and its derivatives are widely used for research  
72 purposes, there is substantial interest in the community for a version of MELTS for other  
73 operating systems and computer architectures. Further, these characteristics are probably the  
74 main reason why MELTS – despite great potential – has not been used more frequently for  
75 teaching purposes. The program PhasePlot (<http://www.phaseplot.org/>) is a modern graphic  
76 interface that allows quick visualization of computations performed using rhyolite-MELTS and  
77 pMELTS [see *Ghiorso and Gualda, 2015*], which makes it an ideal tool for some teaching  
78 purposes. However, PhasePlot is not designed for output of quantitative data, and there are  
79 some limitations to the types of calculations possible, which limits its use for many types of  
80 applications.

81 In this paper we present a new interface for rhyolite-MELTS developed in Microsoft Excel<sup>®</sup>. We  
82 aim to create a more interactive tool, which is easy to use, available to a widespread audience,  
83 and useful for both research and teaching. We first introduce the new interface, and we then  
84 present some examples of applications that can be developed with this interface. Finally, we list  
85 some of the current limitations of the new interface.

## 86 **2. The new interface**

87 MELTS\_Excel uses web services consumed by a VBA backend client; all calculations are  
88 performed on the servers at OFM Research and Excel is used as an interface to send, receive,  
89 and process data exchanged with the server. One key advantage of this approach is that, with  
90 calculations being performed on servers, the only requirement for the end-user machine is for it  
91 to be able to run a version of Excel compatible with REST protocol web services (currently,  
92 Excel 2010 and 2013 for Microsoft Windows operating systems). The interface requires no  
93 installation, allowing use on machines regardless of the administrative privileges of the user;  
94 and there is no need for upgrades in the computation engine, given that all calculations are  
95 performed in a centrally maintained server. Further, the spreadsheet and graphic capabilities of  
96 Excel can be used to create formatted output, including both data and diagrams. The main  
97 disadvantage of the approach is that the interface requires an active internet connection to  
98 communicate with the OFM Research server that performs computations.

99 The interface is contained within a macro-enabled workbook where composition and conditions  
100 are set, which includes several sheets: (1) one sheet for simple calculations and display of live  
101 results, where the user can insert the model input information and trigger simple calculations,  
102 and where a summary of results for any given condition is given; (2) one sheet listing  
103 properties of all phases present at any given condition; (3) one sheet where the user can select  
104 phases to include or exclude in the calculations; and (4) one sheet where the user can specify  
105 sequences of calculations (variable T, P, or both, plus  $f_{O_2}$ ).

106 For calculations at one given condition, the results are immediately displayed within prespecified  
107 fields within the interface. For instance, a user can very rapidly determine the temperature at  
108 which a magma of a given composition is completely molten (i.e. find the liquidus); or  
109 determine which phases are present, in what abundances, their compositions, and their physical  
110 properties (e.g. density, viscosity) at any given combination of temperature, pressure and  
111 oxygen fugacity.

112 It is also possible to combine a sequence of calculations into an evolutionary path. The user can  
113 input starting and ending temperatures and pressures, temperature and pressure steps, and the  
114 prevailing oxidation conditions. Additionally, the user can specify a grid of temperatures and  
115 pressures and calculate a phase diagram in temperature-pressure space. At the conclusion of  
116 the calculations, a series of data sheets and diagrams are created in a separate workbook,

117 which can be saved independently of the interface. This way, the user can save the results  
118 separately from the interface, and the interface can be used repeatedly. The results workbook  
119 includes several sheets, including: (a) sheets with data for each phase (equivalent to [phase  
120 name].tbl files from the GUI); (b) one sheet with data for the whole system (previously  
121 included in melts-liquid.tbl); (c) one sheet with data for total solids (previously included in  
122 melts-liquid.tbl); (d) one sheet including mass, volume, density evolution of each phase, solids,  
123 and whole system as a function of temperature, pressure,  $f_{O_2}$ ; (e) charts with evolution of mass,  
124 volume, density as a function of temperature; (f) charts with compositional evolution of each  
125 phase as a function of temperature; (g) one sheet with affinities for all phases at all  
126 temperatures (useful for calculation of activities relative to mineral saturation); and (h) one  
127 sheet with initial conditions, a reference of the conditions employed in the calculation that can  
128 be used for easy reproduction of the simulation. The routines used to create the output can also  
129 be used to process tbl files returned by the GUI to create equivalent output in Excel.

### 130 **3. Some examples**

131 We present below a few examples that illustrate some of the capabilities of the interface. We  
132 start with examples that reproduce capabilities available in the GUI, and then present examples  
133 of applications facilitated by the new interface.

#### 134 *3.1. A simple calculation*

135 We first present the case of a calculation performed at a single set of conditions (pressure,  
136 temperature, oxygen fugacity) for a given bulk composition. After entering the bulk composition  
137 of interest, the user has a number of options:

- 138 (1) *Equilibrate*: For the bulk composition and set of conditions specified, MELTS calculates  
139 the phases present, their compositions and abundances, as well as the thermodynamic  
140 properties of each phase present;
- 141 (2) *Find liquidus*: For the bulk composition, pressure and oxygen fugacity specified, MELTS  
142 calculates the temperature at which the only remaining phase is liquid; note that MELTS  
143 will try to dissolve all excess water by simply adjusting the temperature, such that  
144 unexpected results may occur for water-oversaturated systems;
- 145 (3) *Find wet liquidus*: Similar to "Find liquidus", except that it allows for excess water to be  
146 present with liquid at the calculated liquidus temperature; the results of both "Find

- 147 liquidus" and "Find wet liquidus" will be the same if the system does not contain free  
148 water at the liquidus;
- 149 (4) *Compute redox*: This option will partition FeO and Fe<sub>2</sub>O<sub>3</sub> based on the specified oxygen  
150 fugacity value; this option is only useful when performing unconstrained redox  
151 calculations, in which case MELTS will use the ratio of Fe<sup>2+</sup>/Fe<sup>3+</sup> to determine the  
152 oxidation state; for calculations in which  $f_{O_2}$  is constrained, MELTS recalculates the  
153 Fe<sup>2+</sup>/Fe<sup>3+</sup> using total Fe, irrespective of how FeO and Fe<sub>2</sub>O<sub>3</sub> are partitioned in the input  
154 values;
- 155 (5) *Normalize*: This recalculates the bulk composition so that the sum of the oxides is 100;  
156 this calculation is immaterial for MELTS, as it assumes that the quantities entered are  
157 grams of each oxide;
- 158 (6) *Normalize anhydrous*: Recalculates the bulk composition so that the sum of oxides,  
159 except water, is 100; this is also immaterial for MELTS and only for the convenience of  
160 the user;
- 161 (7) In the event that the user would like to exclude phases from the calculations, the sheet  
162 "Phases" should be selected, and the box next to each phase to be excluded should be  
163 unchecked.

164 After performing computations with "Equilibrate", "Find liquidus", or "Find wet liquidus", a  
165 summary of the resulting phase properties is displayed in the "Input" sheet, while more detailed  
166 results are displayed in the "Results" tab. Only phases calculated to be present are displayed in  
167 the "Results" sheet, while the affinities [for details, see *Ghiorso and Gualda, 2013*] of each  
168 phase included in the computation are also shown in the "Input" sheet.

169 In Figure 1, we show a screenshot illustrating the results of a calculation performed using  
170 "Equilibrate" for a composition representative of the early-erupted Bishop Tuff [from *Hildreth,*  
171 1979], under water-saturated conditions, and fugacity constrained to the Ni-NiO buffer, at a  
172 temperature of 755 °C and pressure of 175 MPa. Clicking on "Find wet liquidus" would lead to  
173 the temperature being reset to 760.3 °C, with 4.34 g of water present. In this case, "Find  
174 liquidus" would give a physically implausible result given that a substantial amount of excess  
175 water is present at the liquidus. Readjusting H<sub>2</sub>O to 4.00 would cause both "Find liquidus" and  
176 "Find wet liquidus" to calculate a liquidus temperature of 798.9 °C.

177 We expect that using the interface in this mode will greatly facilitate building intuition about  
178 magmas and their properties. This mode will also be useful for selecting parameters for more  
179 complex calculations including sequences and grids described below.

### 180 *3.2. An isobaric sequence of calculations*

181 One of the most common uses of MELTS is to perform isobaric calculations that span a range of  
182 temperatures with a specified temperature step. One of the advantages of the new interface is  
183 that it is straightforward to use simple calculations like those presented above to constrain the  
184 temperature interval over which to perform a sequence of calculations. Using the same  
185 composition and pressure as the example above, we use the “wet liquidus” temperature as the  
186 starting point, and we find that a temperature range of only 10 °C leads to substantial (>50 wt.  
187 %) crystallization [*Gualda et al., 2012a; Gualda et al., 2012b*]. We thus run a sequence of  
188 calculations by filling out the fields in the “Sequences” sheet:

- 189 (1)  $T_1$ ,  $T_2$ , and  $\Delta T$  are the starting temperature, ending temperature, and temperature  
190 step, respectively; we usually use  $T_1$  as the highest temperature, with positive  $\Delta T$   
191 representing a decrement, because a down-temperature calculation is more efficient  
192 computationally; but we emphasize that, at least for equilibrium calculations, the order  
193 in which the calculations are performed is immaterial to the final result, given that each  
194 calculation represents a thermodynamic equilibrium state that is thus independent of the  
195 path leading to that state [*Ghiorso and Gualda, 2015*]; for fractionation or assimilation  
196 calculations, the results are intrinsically dependent upon the sequence of the  
197 calculations;
- 198 (2)  $P_1$ ,  $P_2$ , and  $\Delta P$  are the pressure equivalents of the quantities above; for an isobaric  
199 calculation, both  $P_1$  and  $P_2$  should be set to the same values, while  $\Delta P$  could have any  
200 value;
- 201 (3)  $f_{O_2}$  represents the oxygen fugacity constraints to be used in the calculation; for  
202 constrained calculations (“Constrained” box checked) the user can enter the oxygen  
203 fugacity relative to a variety of buffers, while for unconstrained calculations the FeO and  
204 Fe<sub>2</sub>O<sub>3</sub> values in the “Input” sheet are used to calculate the initial oxygen fugacity  
205 condition, and  $f_{O_2}$  is allowed to vary as the calculations progress [*Ghiorso and Gualda,*  
206 2015];

207 (4) The user would hit the "Run PT Sequence" button to trigger the sequence of  
208 calculations.

209 Using the same composition as the example above, we perform an isothermal calculation from  
210 765 to 755 °C in 0.5 °C steps, at 175 MPa and  $f_{O_2}$  constrained along the Ni-NiO buffer. The  
211 calculations take place over several seconds, with partial updates shown in the "Input" sheet as  
212 the calculation progresses. At the end of the calculation, Excel switches to the resulting  
213 workbook, which includes all the data generated during the calculations and a number of  
214 automatically generated diagrams (some of which are shown in Figure 2).

215 While the example focuses on an isobaric calculation, the interface also allows for isothermal  
216 calculations under variable pressure, as well as calculations in which both temperature and  
217 pressure vary simultaneously. In the latter, the number of steps is chosen between the  
218 temperature and pressure inputs as the one that leads to the larger number of steps, and both  
219 temperature and pressure are varied continuously from T1 and P1 to T2 and P2. In all cases,  
220 the output diagrams are constructed as a function of temperature, which will render them less  
221 useful for isothermal calculations.

222 One of new features of the Excel interface, which distinguishes it from the GUI, is that it  
223 includes in the output the affinities of all phases included in the calculation. The affinities can be  
224 useful in that they relate quite simply to the activities of the corresponding components  
225 [Ghiorso and Gualda, 2013], which can be helpful in the application of Ti-in-quartz, Ti-in-zircon,  
226 and Zr-in-titanite geobarometers [Ferry and Watson, 2007; Hayden et al., 2008; Thomas et al.,  
227 2010; Wark and Watson, 2006]. We demonstrate here the capabilities by calculating  $a_{TiO_2}$  as a  
228 function of temperature from the calculation output. Because both T and  $a_{TiO_2}$  are known, we  
229 can also compute the expected variation in Ti-in-zircon concentration as a function of  
230 temperature (Figure 3). Interestingly, the observed compositions of early-erupted zircon [Reid  
231 et al., 2011] are consistent with crystallization primarily at temperatures below 758 °C, which  
232 matches the temperature interval over which crystallization of early-erupted magmas should  
233 have taken place (see Figure 2).

### 234 3.3. A phase diagram calculation

235 Another new feature in comparison with the GUI is that phase diagram calculations can be  
236 easily performed with the new interface, with a graphic output being generated automatically.  
237 The calculation is also called using the "Sequences" sheet. In this case, the user sets both



238 temperature and pressure intervals and decrements, again with a choice of  $f_{O_2}$  conditions. A  
239 grid of points in temperature-pressure space is created and a full calculation is performed for  
240 each grid point.

241 The main concern with this type of calculation is that the number of calculations increases very  
242 rapidly, and individual phase diagram calculations can take from several minutes to many  
243 hours. Simple calculations, as well as PhasePlot, can be used to constrain the range of  
244 parameters to be used. Phase diagram calculations are performed as a series of isobaric  
245 sequences. To avoid unnecessary calculations, for each sequence (i.e. pressure), calculations  
246 for temperatures greater than the wet liquidus are skipped; similarly, calculations are halted  
247 once the liquid abundance drops below 10 wt. %. This results in dramatic improvements in  
248 speed, and it allows the user to select a wide range of temperatures consistent with the range  
249 of liquidus and solidus temperatures observed for the pressure interval of interest. At the end of  
250 the calculations, the user is presented with a new workbook that includes all the data, and a  
251 diagram displaying the temperatures at which each phase saturates – a phase-in curve – is also  
252 generated; we note that phase-out curves, which would be present if a phase were to become  
253 unstable and completely disappear, are not currently displayed.

254 As an illustrative example, we use again the same early-erupted Bishop Tuff composition, and  
255 we calculate a phase diagram for the temperature range of 810-730 °C, with 1 °C steps, and  
256 the pressure range 250-100 MPa, with 25 MPa steps. Of the 567 points in this grid, only 87  
257 calculations fall at temperatures between the wet liquidus and the 10 wt. % liquid threshold, so  
258 only a relatively small subset of the grid points actually require calculations to be performed. In  
259 the resulting phase diagram (Figure 4), the liquid-in curve represents the lowest superliquidus  
260 temperature on the grid for each pressure. This is also true for the water-in curve in this case,  
261 because we added enough water to the system for it to be water-saturated at the liquidus for  
262 all pressures. It can be seen from this example calculation the nearly invariant nature of the  
263 early-erupted Bishop Tuff compositions, which crystallize over a very narrow temperature  
264 interval [*Gualda and Ghiorso, 2013; Gualda et al., 2012a; Gualda et al., 2012b*].

#### 265 *3.4. A calculation using the rhyolite-MELTS geobarometer*

266 The new interface also makes it possible to apply the rhyolite-MELTS geobarometer [*Gualda*  
267 *and Ghiorso, 2014*], which uses rhyolite-MELTS to calculate the pressure at which a given melt

268 composition can be in simultaneous equilibrium with the expected felsic assemblage (quartz and  
269 feldspars).

270 Parameters for the pressure calculations are set in the same way as for the phase diagram  
271 calculations and, in fact, the calculations are performed in the same way; the only difference is  
272 that an extra sheet is included in the output workbook where the pressure calculations are  
273 made. For proper functioning of the capabilities of this sheet, the user needs to check "Trust  
274 access to the VBA project object model" within the "Macro Settings" of Microsoft Excel "Trust  
275 Center").

276 The composition used in the examples above is representative of both early-erupted Bishop Tuff  
277 bulk rocks [*Hildreth, 1979*] and quartz-hosted glass inclusions [*Anderson et al., 2000*]. Early-  
278 erupted magmas are characterized by the presence of quartz, sanidine, and plagioclase  
279 [*Anderson et al., 2000; Gualda and Ghiorso, 2013; Hildreth, 1979*]. The pressure calculations  
280 (Figure 4) show that all three phases are in simultaneous equilibrium at pressures of ~170 MPa  
281 (Figure 4b). Even if melt inclusions were entrapped prior to saturation in both feldspars, the  
282 estimated saturation pressure would still be the same (Figure 4c) [for more details, see *Gualda*  
283 *and Ghiorso, 2014*].

#### 284 **4. Some current limitations**

285 MELTS\_Excel is in active development, and not all the envisioned functionality is implemented.  
286 As such, there are some current limitations:

- 287 (1) MELTS\_Excel currently only works with rhyolite-MELTS, and there is no interface with  
288 pMELTS (rhyolite-MELTS effectively replace MELTS, given that the calibration for mafic  
289 systems is identical, and it takes advantage of the much improved calculation algorithms  
290 included in rhyolite-MELTS [*Ghiorso, 2013*]);
- 291 (2) Only equilibrium mode calculations are currently implemented; implementation of  
292 fractionation modes is planned for the near future;
- 293 (3) Only calculations using pressure and temperature (as opposed to entropy and volume)  
294 as independent variables (i.e. Gibbs free-energy minimization and related  $f_{O_2}$ -constrained  
295 Korzhinskii potential minimization [*Ghiorso and Gualda, 2015*]) are currently  
296 implemented, which precludes isenthalpic or isochoric calculations available through the  
297 existing MELTS GUI; we intend to eventually implement such capabilities;
- 298 (4) No assimilation mode is currently implemented;

299 We envision that, for most users, the new interface will replace the existing GUI. However, one  
300 of the hallmarks of the GUI is its flexibility and the ability to simulate complex evolution  
301 histories. In many ways, the new Excel interface is currently less flexible, which may cause  
302 some advanced users to prefer the GUI for specific calculations. In these cases, the ability to  
303 import and process tbl files to generate equivalent output (under "Tools" tab) may be a useful  
304 functionality of MELTS\_Excel.

## 305 **5. Conclusions**

306 In this paper we present MELTS\_Excel, a new interface for rhyolite-MELTS based on Microsoft  
307 Excel. It utilizes web services to perform calculations on a remote server at OFM Research and  
308 deliver results to the user in an Excel workbook. It takes advantage of spreadsheet and graphic  
309 capabilities of Microsoft Excel to simplify both data input and output. Due to differences in  
310 capability of web services available in the various versions of Excel, MELTS\_Excel currently only  
311 works on versions 2010 and 2013 of Microsoft Excel for Windows.

312 The interface is contained within a macro-enabled workbook, which includes editable cells  
313 where the user can insert the model input information. Results of simple calculations are shown  
314 immediately within the interface itself.

315 It is also possible to combine a sequence of calculations into an evolutionary path. The user can  
316 input starting and ending temperatures and pressures, temperature and pressure steps, and the  
317 prevailing oxidation conditions, and the program will perform the calculations showing the  
318 magma properties at every step; at the conclusion of the calculations, a series of data sheets  
319 and diagrams are created in a separate workbook, which can be saved independently of the  
320 interface.

321 Additionally, the user can specify a grid of temperatures and pressures and calculate a phase  
322 diagram showing the conditions at which different phases are present. Pressure estimation  
323 using the rhyolite-MELTS geobarometer is also possible using the interface.

324 The main advantages of this new interface are that it is simple to use and flexible. The interface  
325 is built on a popular platform and which is widely available. The interface requires no  
326 installation and it is distributed for free. The main drawback is that operation of the workbook  
327 requires an internet connection. The interface is actively being developed, so not all features of  
328 the GUI are currently implemented in MELTS\_Excel.

329 We expect that the new interface will facilitate the use of rhyolite-MELTS, particularly for the  
330 novice user, but also for users performing a large number of simulations. We hope that  
331 MELTS\_Excel will also facilitate the use of MELTS for teaching purposes.

## 332 **6. Acknowledgements**

333 MELTS\_Excel can be downloaded for free from: <http://melts.ofm-research.org>. Financial  
334 support was provided by NSF (EAR-1321806, EAR-1151337, EAR-0948528 to Gualda and EAR-  
335 0948734, EAR-1321924 to Ghiorso) and by a Vanderbilt University Discovery Grant to Gualda.

336

337 **7. References**

- 338 Anderson, A. T., A. M. Davis, and F. Q. Lu (2000), Evolution of Bishop Tuff rhyolitic magma  
339 based on melt and magnetite inclusions and zoned phenocrysts, *Journal of Petrology*, *41*(3),  
340 449-473.
- 341 Asimow, P. D., and M. S. Ghiorso (1998), Algorithmic modifications extending MELTS to  
342 calculate subsolidus phase relations, *American Mineralogist*, *83*(9-10), 1127-1132.
- 343 Ferry, J. M., and E. B. Watson (2007), New thermodynamic models and revised calibrations for  
344 the Ti-in-zircon and Zr-in-rutile thermometers, *Contributions to Mineralogy and Petrology*,  
345 *154*(4), 429-437.
- 346 Ghiorso, M. S. (1997), Thermodynamic models of igneous processes, *Annual Review of Earth  
347 and Planetary Sciences*, *25*, 221-241.
- 348 Ghiorso, M. S. (2013), A globally convergent saturation state algorithm applicable to  
349 thermodynamic systems with a stable or metastable omni-component phase, *Geochimica Et  
350 Cosmochimica Acta*, *103*, 295-300.
- 351 Ghiorso, M. S., and R. O. Sack (1995), Chemical mass-transfer in magmatic processes. 4. A  
352 revised and internally consistent thermodynamic model for the interpolation and extrapolation  
353 of liquid-solid equilibria in magmatic systems at elevated-temperatures and pressures,  
354 *Contributions to Mineralogy and Petrology*, *119*(2-3), 197-212.
- 355 Ghiorso, M. S., and G. A. R. Gualda (2013), A method for estimating the activity of titania in  
356 magmatic liquids from the compositions of coexisting rhombohedral and cubic iron-titanium  
357 oxides, *Contributions To Mineralogy and Petrology*, *165*(1), 73-81.
- 358 Ghiorso, M. S., and G. A. R. Gualda (2015), Chemical thermodynamics and the study of  
359 magmas, in *Encyclopedia of Volcanoes*, edited by H. Sigurdsson, p. in press.
- 360 Ghiorso, M. S., M. M. Hirschmann, P. W. Reiners, and V. C. Kress (2002), The pMELTS: A  
361 revision of MELTS for improved calculation of phase relations and major element partitioning  
362 related to partial melting of the mantle to 3 GPa, *Geochemistry Geophysics Geosystems*, *3*.
- 363 Gualda, G. A. R., and M. S. Ghiorso (2013), The Bishop Tuff giant magma body: an alternative  
364 to the Standard Model, *Contributions to Mineralogy and Petrology*, *166*(3), 755-775.
- 365 Gualda, G. A. R., and M. S. Ghiorso (2014), Phase-equilibrium geobarometers for silicic rocks  
366 based on rhyolite-MELTS. Part 1: Principles, procedures, and evaluation of the method,  
367 *Contributions to Mineralogy and Petrology C7 - 1033*, *168*(1), 1-17.
- 368 Gualda, G. A. R., M. S. Ghiorso, R. V. Lemons, and T. L. Carley (2012a), Rhyolite-MELTS: A  
369 modified calibration of MELTS optimized for silica-rich, fluid-bearing magmatic systems, *Journal  
370 of Petrology*, *53*(5), 875-890.
- 371 Gualda, G. A. R., A. S. Pamukcu, M. S. Ghiorso, A. T. Anderson, Jr., S. R. Sutton, and M. L.  
372 Rivers (2012b), Timescales of quartz crystallization and the longevity of the Bishop giant  
373 magma body, *Plos One*, *7*(5), e37492.

- 374 Hayden, L. A., E. B. Watson, and D. A. Wark (2008), A thermobarometer for sphene (titanite),  
375 *Contributions to Mineralogy and Petrology*, 155(4), 529-540.
- 376 Hildreth, W. (1979), The Bishop Tuff: Evidence for the origin of compositional zonation in silicic  
377 magma chambers, *Geological Society of America Special Paper*, 180, 43-75.
- 378 Reid, M. R., J. A. Vazquez, and A. K. Schmitt (2011), Zircon-scale insights into the history of a  
379 Supervolcano, Bishop Tuff, Long Valley, California, with implications for the Ti-in-zircon  
380 geothermometer, *Contributions to Mineralogy and Petrology*, 161(2), 293-311.
- 381 Thomas, J. B., E. B. Watson, F. S. Spear, P. T. Shemella, S. K. Nayak, and A. Lanzirotti (2010),  
382 TitaniQ under pressure: the effect of pressure and temperature on the solubility of Ti in quartz,  
383 *Contributions to Mineralogy and Petrology*, 160(5), 743-759.
- 384 Wark, D. A., and E. B. Watson (2006), TitaniQ: a titanium-in-quartz geothermometer,  
385 *Contributions to Mineralogy and Petrology*, 152(6), 743-754.
- 386
- 387
- 388

389 **8. Figure captions**

390 **Figure 1.** Screenshot showing the "Input" sheet of MELTS\_Excel, where the system  
391 composition is defined, as well as temperature, pressure and oxygen fugacity conditions for  
392 simple calculations. Several buttons that trigger sample calculations can be seen. The result of  
393 an "Equilibrate" calculation at the conditions listed are displayed on the right portion, including  
394 the names, abundances and compositions of phases present, as well as the affinities of all  
395 phases that are not present but which are included in the calculation. More detailed results are  
396 presented in the "Results" sheet.

397 **Figure 2.** Graphics displaying some of the results of an isobaric sequence of calculations. The  
398 composition is the same as shown in **Figure 1**. The temperature range is 765-755 °C, in 0.5 °C  
399 steps, at 175 MPa, with  $f_{O_2}$  constrained along the Ni-NiO buffer. *Top:* Variation in mass as a  
400 function of temperature for all phases present, for all solids, and for the whole system. *Middle:*  
401 Variation in liquid composition as a function of temperature; note that SiO<sub>2</sub> is shown on a  
402 different vertical scale (to the right) than the other oxides. *Bottom:* Variation in the composition  
403 of feldspars as a function of temperature; the highest temperature feldspar appears at 760 °C,  
404 while a lower temperature feldspar saturates at 759.9 °C; the zigzag lines demonstrate the  
405 coexistence of two feldspars within that temperature range.

406 **Figure 3.** Example of the use of rhyolite-MELTS to calculate  $a_{TiO_2}$  and Ti-in-zircon as a function  
407 of temperature using the variation in the affinity of rutile as a function of temperature. *Top:*  
408 Variation in  $a_{TiO_2}$  as a function of temperature calculated using the relationship shown on the  
409 right panel [see *Ghiorso and Gualda, 2013*]. *Bottom:* Variation in Ti-in-zircon as a function of  
410 temperature calculated using the Ti-in-zircon calibration of Ferry & Watson [2007]; panel on the  
411 right shows histogram of Ti abundances in zircon from early-erupted Bishop Tuff [*Reid et al.,*  
412 2011], on the same vertical scale as the plot on the left; the histogram shows that the vast  
413 majority of zircons are expected to have crystallized at temperatures below 758 °C, consistent  
414 with the range of temperatures over which crystallization of early-erupted magmas should have  
415 taken place (see **Figure 2**).

416 **Figure 4.** Example calculation of a phase diagram and application of the rhyolite-MELTS  
417 geobarometer. *Top:* Phase diagram calculated for the same composition as in the prior  
418 examples, over a temperature range of 810-730 °C (1 °C steps) and a pressure range of 250-  
419 100 MPa (25 MPa steps). *Bottom:* Diagrams showing the application of the rhyolite-MELTS

420 geobarometer; left panel shows calculation of the pressure at which quartz and two feldspars  
421 are expected to be in equilibrium with the input glass composition; right panel shows calculation  
422 of the pressure at which quartz and one feldspar are expected to be in equilibrium with the  
423 input glass compositions [for further details, see *Gualda and Ghiorso, 2014*].



	A	B	C	D	E	F	G	H	I	J
1		<b>System</b>		<b>System</b>		<b>Unit</b>		<b>System</b>	<b>109.80</b>	
2	SiO <sub>2</sub>	77.700		P	175	MPa		Liquid		12.66
3	TiO <sub>2</sub>	0.080		T	755.0	C		Solids		97.15
4	Al <sub>2</sub> O <sub>3</sub>	12.500		log fO <sub>2</sub>	0.00	ΔNNO				
5	Fe <sub>2</sub> O <sub>3</sub>	0.192		<input checked="" type="checkbox"/> fO <sub>2</sub> constrained						
6	Cr <sub>2</sub> O <sub>3</sub>							<b>Phase</b>	<b>Mass</b>	<b>Formula</b>
7	FeO	0.487						liquid		12.66 SiO <sub>2</sub> 0.77 TiO <sub>2</sub> 0.00 Al <sub>2</sub> O <sub>3</sub> 0.12 Fe <sub>2</sub> O <sub>3</sub> 0.00 FeO 0.01 MgO 0.00 CaO 0.01 Na <sub>2</sub> O 0.04 K <sub>2</sub> O 0.05 H <sub>2</sub> O 0.05
8	MnO							feldspar		44.65 K <sub>0.51</sub> Na <sub>0.47</sub> Ca <sub>0.02</sub> Al <sub>1.02</sub> Si <sub>1.98</sub> O <sub>4</sub>
9	MgO	0.030						quartz		30.77 SiO <sub>2</sub>
10	NiO							feldspar		12.19 K <sub>0.15</sub> Na <sub>0.17</sub> Ca <sub>0.08</sub> Al <sub>1.08</sub> Si <sub>1.92</sub> O <sub>4</sub>
11	CoO							water		8.88 H <sub>2</sub> O
12	CaO	0.430						spinel		0.66 Fe <sup>1.18</sup> Mg <sub>0.06</sub> Fe <sup>1.42</sup> Al <sub>0.07</sub> Cr <sub>0.00</sub> Ti <sub>0.26</sub> O <sub>4</sub>
13	Na <sub>2</sub> O	3.990						<b>Potential Phase</b>	<b>Affinity (kJ)</b>	<b>Formula</b>
14	K <sub>2</sub> O	4.890						orthopyroxene		0.28 opx Na <sub>0.00</sub> Ca <sub>0.99</sub> Fe <sup>1.00</sup> Mg <sub>0.11</sub> Fe <sup>1.00</sup> Ti <sub>0.01</sub> Al <sub>0.55</sub> Si <sub>1.44</sub> O <sub>6</sub>
15	P <sub>2</sub> O <sub>5</sub>							rhm-oxide		0.95 Mn <sub>0.05</sub> Fe <sup>1.00</sup> Mg <sub>0.95</sub> Fe <sup>1.00</sup> Al <sub>0.00</sub> Ti <sub>0.88</sub> O <sub>3</sub>
16	H <sub>2</sub> O	9.500						clinopyroxene		1.50 cpx Na <sub>0.00</sub> Ca <sub>0.99</sub> Fe <sup>1.00</sup> Mg <sub>0.99</sub> Fe <sup>1.00</sup> Al <sub>0.01</sub> Al <sub>0.50</sub> Si <sub>1.50</sub> O <sub>6</sub>
17	CO <sub>2</sub>							biotite		1.53 K(Fe <sup>1.00</sup> Mg <sub>0.00</sub> ) <sub>3</sub> AlSi <sub>3</sub> O <sub>10</sub> (OH) <sub>2</sub>
18	SO <sub>2</sub>							tridymite		2.15 SiO <sub>2</sub>
19	Cl <sub>2</sub> O-1							crystalite		2.21 SiO <sub>2</sub>
20	F <sub>2</sub> O-1							olivine		3.71 (Ca <sub>0.00</sub> Mg <sub>0.00</sub> Fe <sup>1.00</sup> Mn <sub>0.98</sub> Co <sub>0.01</sub> Ni <sub>0.01</sub> ) <sub>2</sub> SiO <sub>4</sub>
21				Success: Equilibrate				cummingtonite		7.00 (Fe <sup>1.00</sup> Mg <sub>1.00</sub> ) <sub>7</sub> Si <sub>8</sub> O <sub>22</sub> (OH) <sub>2</sub>
22								rutile		7.10 TiO <sub>2</sub>
23								feralite		8.33 Fe <sub>2</sub> SiO <sub>4</sub>
24								garnet		11.68 (Ca <sub>0.11</sub> Fe <sup>1.00</sup> Mg <sub>0.00</sub> ) <sub>3</sub> Al <sub>2</sub> Si <sub>3</sub> O <sub>12</sub>
25								sillimanite		15.20 Al <sub>2</sub> SiO <sub>5</sub>
26								sphene		15.36 CaTiSiO <sub>5</sub>
27								corundum		15.59 Al <sub>2</sub> O <sub>3</sub>
28								ortho-oxide		18.34 Fe <sup>1.00</sup> Mg <sub>0.00</sub> Fe <sup>1.00</sup> Ti <sub>1.00</sub> O <sub>3</sub>
29								muscovite		25.83 KAl <sub>2</sub> Si <sub>2</sub> AlO <sub>10</sub> (OH) <sub>2</sub>
30								perovskite		29.83 CaTiO <sub>3</sub>
31								hornblende		34.65 NaCa <sub>2</sub> Mg <sub>3.98</sub> Fe <sub>2.02</sub> Al <sub>1.00</sub> Fe <sub>3.00</sub> Al <sub>2</sub> Si <sub>6</sub> O <sub>22</sub> (OH) <sub>2</sub>
32								nepheline		43.62 neph Na <sub>0.07</sub> K <sub>0.92</sub> Ca <sub>0.00</sub> [Al <sub>0.02</sub> Al <sub>3.98</sub> Si <sub>4.02</sub> O <sub>16</sub>
33								mellilite		44.78 Na <sub>0.00</sub> Ca <sub>2.00</sub> Al <sub>0.99</sub> Mg <sub>0.06</sub> Fe <sub>0.05</sub> Si <sub>1.74</sub> O <sub>7</sub>
34								aenigmatite		45.80 Na <sub>2</sub> Fe <sub>3</sub> TiSi <sub>4</sub> O <sub>20</sub>
35								alloy-solid		65.90 solid Fe <sub>1.00</sub> Ni <sub>0.00</sub>
36								alloy-liquid		70.50 liquid Fe <sub>1.00</sub> Ni <sub>0.00</sub>
37								aegirine		141.08 NaFeSi <sub>2</sub> O <sub>6</sub>
38										

Equilibrate

---

Find Liquidus

---

Find Wet Liquidus

---

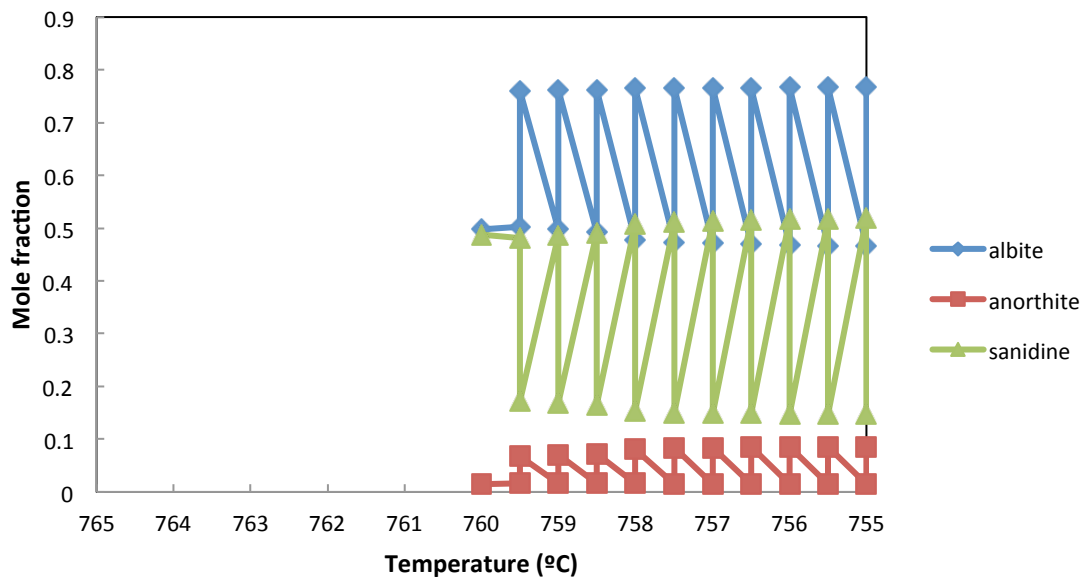
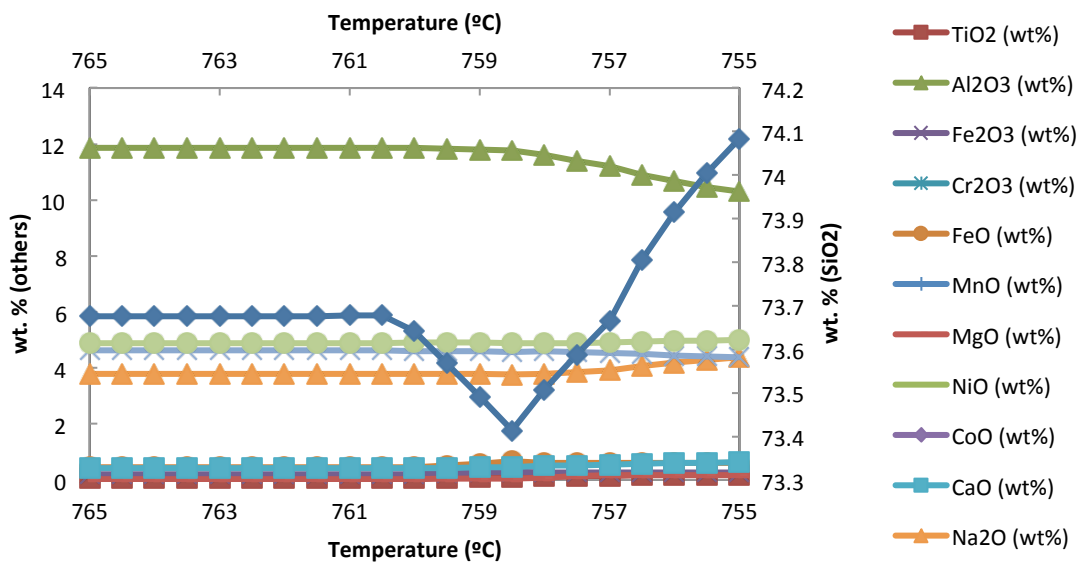
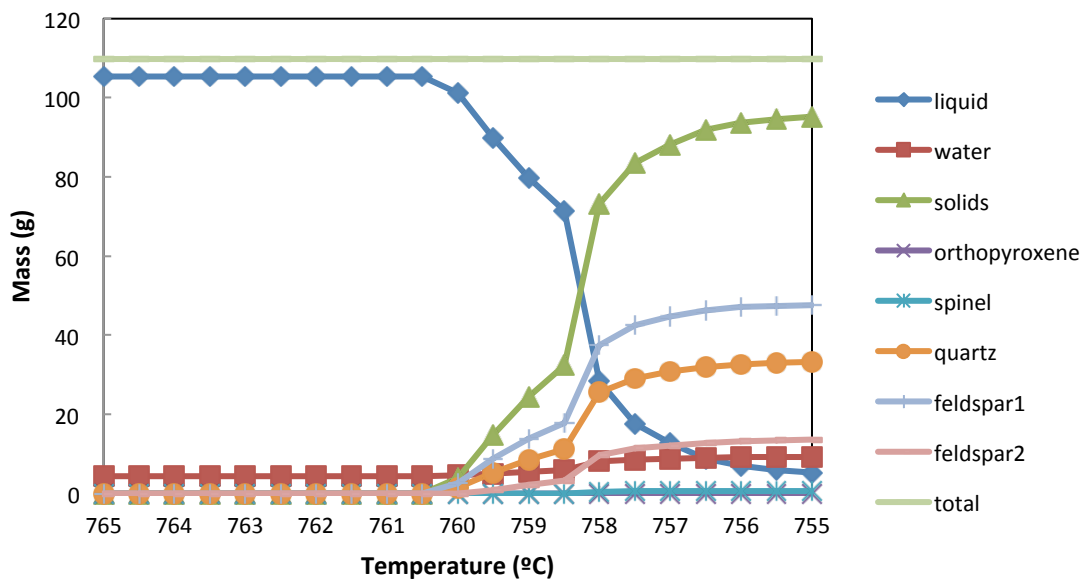
Compute Redox

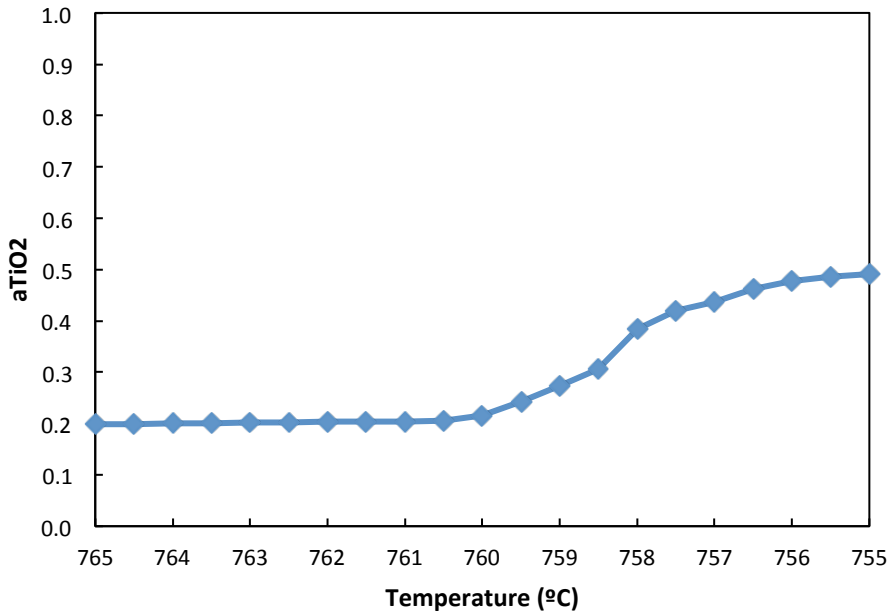
---

Normalize

---

Normalize Anhydrous



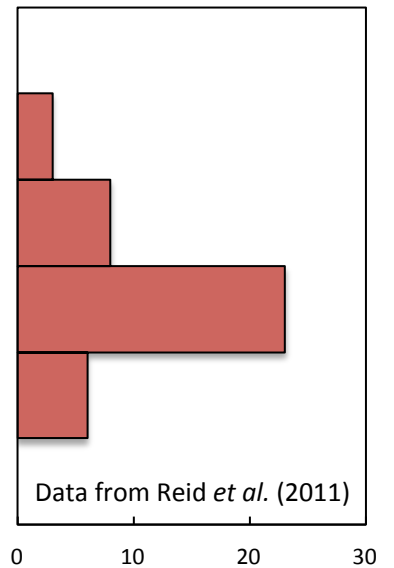
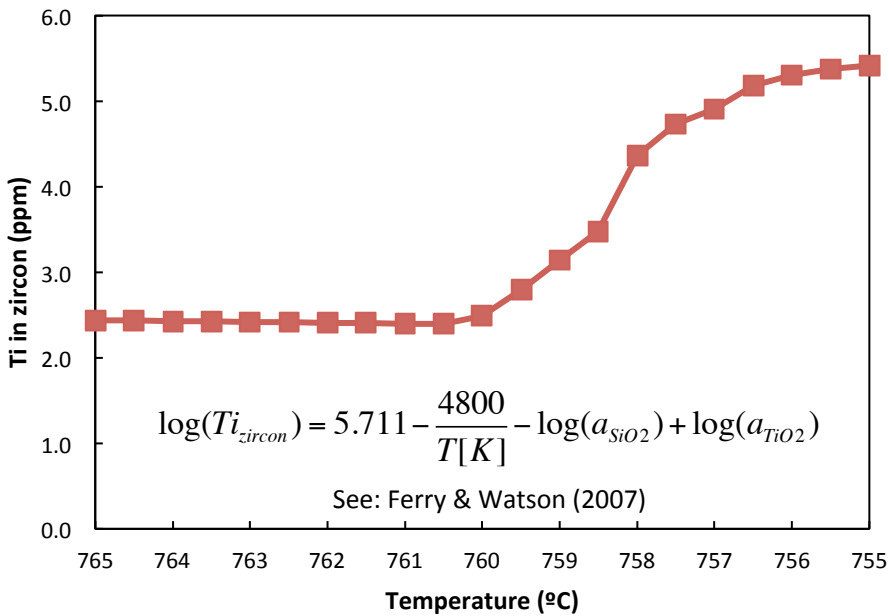


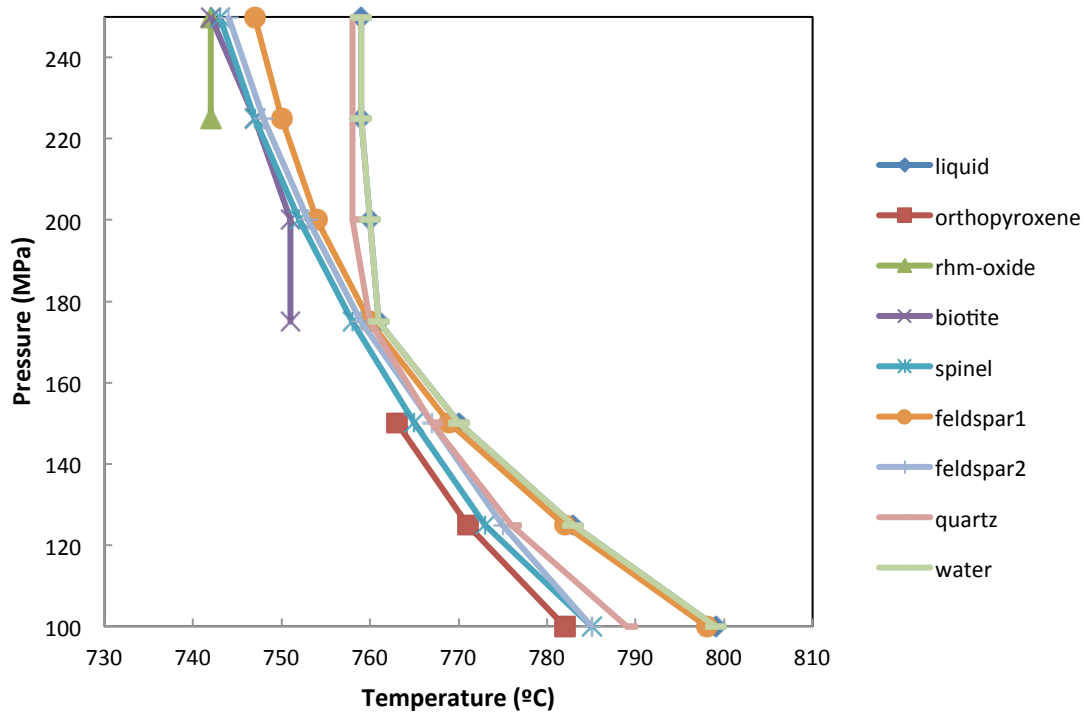
Chemical affinity for rutile saturation

$$a_{TiO_2}^{liquid-rutile} = \exp\left(-\frac{A_{rutile}}{RT}\right)$$

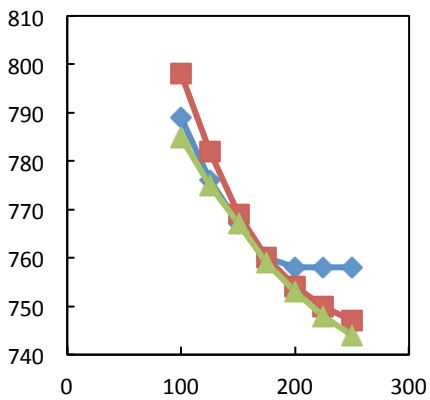
Activity of TiO<sub>2</sub> referenced to rutile saturation

See: Ghiorso & Gualda (2013)





**Quartz+2 Feldspars**



**Quartz+1 Feldspar**

